MATHEMATICS OF COMPUTATION
Volume 78, Number 268, October 2009, Pages 1869–1890
S 0025-5718(09)02246-7
Article electronically published on May 5, 2009

MULTILEVEL FINITE ELEMENT PRECONDITIONING FOR $\sqrt{3}$ REFINEMENT

JAN MAES AND PETER OSWALD

ABSTRACT. We develop a BPX-type multilevel method for the numerical solution of second order elliptic equations in $\mathbb{R}^2$ using piecewise linear polynomials on a sequence of triangulations given by regular $\sqrt{3}$ refinement. A multilevel splitting of the finest grid space is obtained from the nonnested sequence of spaces on the coarser triangulations using prolongation operators based on simple averaging procedures. The main result is that the condition number of the corresponding BPX preconditioned linear system is uniformly bounded independent of the size of the problem. The motivation to consider $\sqrt{3}$ refinement stems from the fact that it is a slower topological refinement than the usual dyadic refinement, and that it alternates the orientation of the refined triangles. Therefore we expect a reduction of the amount of work when compared to the classical BPX preconditioner, although both methods have the same asymptotical complexity. Numerical experiments confirm this statement.

1. INTRODUCTION

In this paper we propose an optimal multilevel preconditioner of BPX-type for the solution of second order elliptic problems using nonnested spaces of linear elements on triangulations of a two-dimensional bounded domain, where the triangulations are obtained by regular $\sqrt{3}$ refinement. In order to develop the theory we will restrict ourselves to the most simple elliptic equation: the Poisson problem

$$-\Delta u = f \quad \text{in} \quad \Omega, \qquad u = 0 \quad \text{on} \quad \partial\Omega, \tag{1.1}$$

where Ω is a polygonal domain in $\mathbb{R}^2$ and $\partial\Omega$ is its boundary. The BPX preconditioner [4] was originally introduced for linear elements on a nested sequence of quasi-uniform triangulations Δ_j of the domain Ω, where the triangulation Δ_j has mesh-size $h_j \sim 2^{-j}$ and has been obtained from some initial triangulation Δ_0 by j steps of a regular dyadic refinement process. Roughly speaking, the BPX preconditioner stresses the fact that discretization matrices of elliptic problems with respect to the frame of all standard nodal basis functions on all resolution levels $0 \le j \le J$ are significantly better conditioned than those arising from the standard nodal basis on the finest level J. It has been shown in [13] that the condition number of the BPX preconditioned system for linear elements on dyadically refined triangulations is uniformly bounded in the size of the problem. This estimate results in a preconditioned conjugate gradient method for solving (1.1) which is optimal in the following sense: if the solution can be approximated to accuracy

Received by the editor June 1, 2007 and, in revised form, August 30, 2008.
2000 *Mathematics Subject Classification.* Primary 65F10, 65F35, 65N30, 35J20.
Key words and phrases. Multilevel preconditioning, $\sqrt{3}$ subdivision, elliptic equations.

$\mathcal{O}(h_J)$ in the energy norm by a continuous piecewise linear function on Δ_J, then the BPX preconditioned conjugate gradient method (applied in conjunction with nested iteration) constructs an approximation with the same asymptotic accuracy in only $\mathcal{O}(n_J)$ operations, with n_J the number of standard nodal basis functions on the finest resolution level J.

Before introducing the BPX method for linear finite element discretizations on quasi-uniform triangulations obtained by regular $\sqrt{3}$ refinement, we first explain how $\sqrt{3}$ refinement works. It was originally introduced by Kobbelt [10] with applications to surface design in CAGD in mind, and we present it in a version adapted to our needs, which we called regularized $\sqrt{3}$ refinement. We start from an initial conforming triangulation Δ_0 of Ω. For every triangle in Δ_0 we choose a new vertex inside this triangle and connect it with the three old vertices of the triangle. Flipping the original edges then yields the new triangulation Δ_1. Note that Δ_1 is not contained in Δ_0. When we apply another step of $\sqrt{3}$ refinement to Δ_1, we arrive at Δ_2, which, roughly speaking, is equivalent to the result of one step of triadic refinement, i.e., each original triangle is replaced by 9 new triangles. See Figure 1 for an illustration of these geometric rules in the case of a uniform partition, where the inserted point is always chosen at the barycenter of the triangle. For the analysis in this paper, and to avoid possible degeneracies, from now on the following regularized version of the $\sqrt{3}$ refinement scheme is adopted. In the *odd* refinement step $\Delta_{2j} \to \Delta_{2j+1}$ the inserted vertices are the triangle barycenters while in the *even* refinement step $\Delta_{2j+1} \to \Delta_{2(j+1)}$ the points $P_{e,-} := (2P_- + P_+)/3$, $P_{e,+} := (P_- + 2P_+)/3$ on an edge e with endpoints P_-, P_+ from Δ_{2j} are inserted. We refer to Figure 2 for a visualization of the notation that is used throughout this paper. The boundary treatment is implemented by extending the triangulation as follows: To every boundary edge e of Δ_{2j}, we will attach a virtual exterior triangle $T_{e,-}$ (take the only triangle $T_{e,+}$ in Δ_{2j} that is attached to e, and reflect it about the edge midpoint M_e), and then apply an odd and an even refinement step to the extended triangulation as described above. To obtain Δ_{2j+1} and $\Delta_{2(j+1)}$, we intersect the obtained (extended) triangulations with Ω. In Δ_{2j+1}, half-edges that connect with the barycenters of virtual boundary triangles are removed to avoid the appearance of an additional ghost vertex at the midpoint of the boundary edge (which does not appear in Δ_{2j+2}). Figure 3 depicts the $\sqrt{3}$ refinement process near the boundary. For all this to work in agreement with the geometric idea of $\sqrt{3}$ refinement, one has to require that the union of two triangles $T_{e,\pm}$ attached to an interior edge e in Δ_0 is a strictly convex quadrilateral (a sufficient condition for this to hold is that the maximal interior angle of any triangle in Δ_0 is less than $\pi/2$).

The following properties of regularized $\sqrt{3}$ refinement are then obvious:

a) The sequence $\{\Delta_j\}$ is automatically regular and quasi-uniform, with typical element size parameter $h_j \sim 3^{-j/2}$ and with regularity constants depending solely on the initial triangulation.
b) The subsequence $\{\Delta_{2j}\}$ is obtained by triadic refinement from the initial triangulation Δ_0.
c) The ladder of linear finite element subspaces

$$S_0 \to S_1 \to \cdots \to S_j \to \cdots \to S_J \to \cdots \tag{1.2}$$

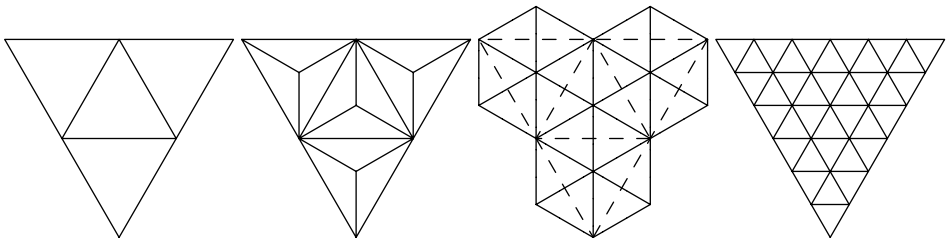

FIGURE 1. $\sqrt{3}$ refinement of a uniform triangulation. One new vertex per triangle is computed, this vertex is connected with the vertices of the triangle, and the edges between old vertices are flipped. Applying the $\sqrt{3}$ refinement twice yields a triadic refinement.

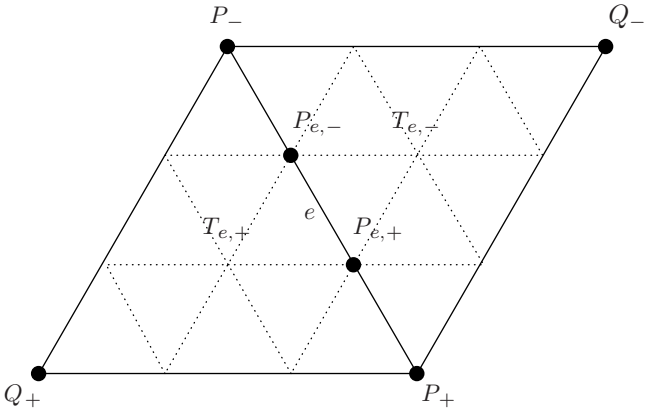

FIGURE 2. Visualization of the notation for vertices and triangles in the neighborhood of some edge e.

in $H_0^1(\Omega)$ associated with $\{\Delta_j\}$ is only partially nested. On the one hand, we have

$$S_0 \subset S_2 \subset \cdots \subset S_{2j} \subset \cdots \tag{1.3}$$

for even levels due to b); on the other hand, we obviously have $S_{2j} \not\subset S_{2j+1}$ and $S_{2j+1} \not\subset S_{2(j+1)}$.

Thus, the construction of multilevel, resp. multigrid, algorithms using the ladder $\{S_j\}$ requires some care; in particular, it requires nontrivial prolongation operators $I_j : S_{j-1} \to S_j$, $j \geq 1$, to connect between the discretizations on subsequent levels $j-1$ and j. In this paper, we consistently use interpolation at the old vertices and linear averaging at the newly inserted vertices for defining the I_j. I.e., if P is a new vertex in Δ_j, and P_i, $i = 1, 2, 3$, denote the vertices of the corresponding triangle T from Δ_{j-1}, then

$$I_j v_{j-1}(P) = \frac{1}{3} \sum_{i=1}^{3} v_{j-1}(P_i), \tag{1.4}$$

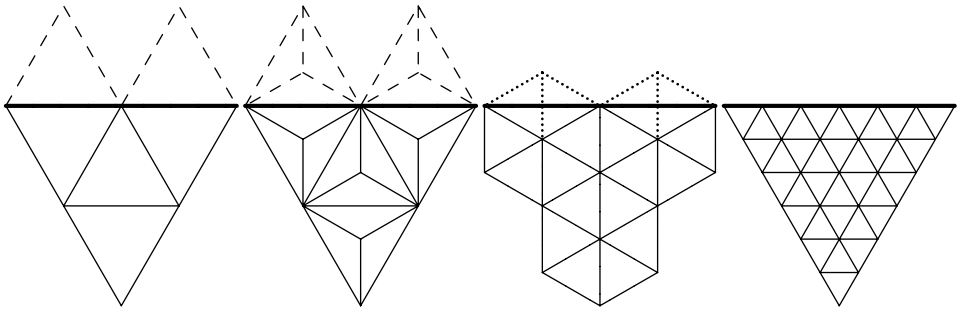

FIGURE 3. $\sqrt{3}$ refinement near the boundary. We extend the triangulation Δ_{2j} by attaching virtual exterior triangles to the boundary. After applying an odd or both an odd and even refinement step to the extended triangulation we intersect the obtained extended triangulation with Ω to obtain Δ_{2j+1} resp. Δ_{2j+2}. If only an odd refinement step has been applied we also remove any half-edges that connect with the barycenters of the virtual boundary triangles.

while $I_j v_{j-1}(P_i) = v_{j-1}(P_i)$ for the vertices from Δ_{j-1}. New boundary vertices appear only in even refinement steps; for them the above rule is modified: The values at the two new boundary vertices $P'_{\pm}$ in Δ_{2j} located on a boundary edge from Δ_{2j-2} are obtained by linear interpolation along the boundary edge, i.e., from the values at the endpoints $P_{\pm}$ belonging to Δ_{2j-2} (and Δ_{2j-1}). While for odd j this definition is in agreement with local linear interpolation (i.e., $I_{2j+1} v_{2j}(P) = v_{2j}(P)$ at the newly inserted barycenters), for even j this definition only guarantees local reproduction of constants. Consequently, $I_{2j+2} I_{2j+1} : S_{2j} \to S_{2j+2}$ is different from the natural injection for the nested subspaces $S_{2j} \subset S_{2j+2}$; the resulting scheme associated with triadic refinement is not covered by standard multigrid theory, and thus needs special consideration. The motivation for using the sequence (1.2) instead of the traditional nested sequence of linear finite element spaces obtained by regular dyadic refinement stems from the following considerations. First of all, $\sqrt{3}$ refinement is a slower topological refinement than the usual dyadic split operation. This implies that we can have more levels of refinement if a prescribed target complexity of the finite element space must not be exceeded. Furthermore, $\sqrt{3}$ refinement locally alternates the orientation of triangles in each step. These properties potentially might have the advantage of reducing the amount of work in an adaptive strategy, since certain features or singularities that are not aligned with the initial triangulation might be detected more quickly. Although out of the scope of this paper, the $\sqrt{3}$ splitting operation easily enables locally adaptive refinement, and the size of the surrounding mesh area which is affected by such selective refinement is smaller than for the dyadic split operation; see [10, 11]. The work in this paper may also be motivated from another perspective. Because of the nonnestedness of the subsequent finite element spaces, this work fits into the theory of multigrid preconditioners for nonconforming finite element discretizations which has been investigated in, e.g., [2, 5, 6, 7, 8, 12, 15, 16]. Therefore it can be considered as another case study in the construction of optimal multilevel preconditioners with nonnested discretization spaces.

The remainder of the paper is organized as follows. In Section 2 we give a brief review of the theory of multilevel splittings related to nonnested spaces. The proof of the main result of this paper (the proof of a norm equivalence for the ladder $\{S_j\}$ and the prolongations $\{I_j\}$ yielding an optimal condition number estimate for the associated multilevel preconditioner) is carried out in Section 3 and consists of two essential parts. First, we prove modified Jackson and Bernstein estimates for the spaces S_{2j} corresponding to nested triadically refined triangulations of the whole $\mathbb{R}^2$, and we establish the desired norm equivalence for this special case (see Proposition 2.2 in Section 2). In the second step, we extend the results for $\mathbb{R}^2$ to the general case of bounded polygonal domains, the case of homogeneous Dirichlet boundary conditions, and to the full sequence $\{S_j\}$ (see the main result of this paper, Theorem 3.5, in Section 3.3). Finally, in Section 4, we provide numerical evidence of the optimality of the derived multilevel preconditioner based on $\sqrt{3}$ refinement, and we compare it with the standard BPX preconditioner for dyadic refinement from [4]. As it turns out, for problems of comparable size, the $\sqrt{3}$ approach needs fewer iterations than the standard BPX preconditioner.

2. Multilevel splittings related to nonnested spaces

We start with stating some basic facts on the variational theory of multilevel preconditioning with nonnested spaces; a more detailed treatment can be found in, e.g., [16]. We restrict ourselves to symmetric elliptic variational problems in Sobolev spaces of integer smoothness order $k > 0$. Let

$$V_0 \to V_1 \to \cdots \to V_j \to \cdots \to V_J$$

be a sequence of (nonnested) finite element subspaces with respect to an increasing sequence of triangulations obtained by regular ρ-adic refinement. The spaces V_j are comprised of piecewise polynomials of degree d with $d > k - 1$, and we assume that they allow for local reproduction of polynomials of total degree $\leq d$. The main difficulty is the fact that, in general, $V_{j-1} \not\subset V_j$. Suppose that a given symmetric positive definite variational problem in the Sobolev space $H^k(\Omega)$ is suitably approximated by a sequence of variational problems in these finite element subspaces V_j:

$$\text{Find } u_j \in V_j \text{ such that } a_j(u_j, v_j) = (f, v_j) \quad \forall v_j \in V_j. \tag{2.1}$$

Here we will assume that the symmetric positive definite bilinear forms $a_j(\cdot,\cdot)$ are suitable discretizations of a bilinear form $a(\cdot,\cdot)$ on $H^k(\Omega)$, and that the ellipticity condition

$$a_j(u_j, u_j) \sim \|u_j\|_{k,j}^2 \tag{2.2}$$

holds with constants independent of j. In order to avoid the repeated use of generic but unspecified constants, we always mean by $a \sim b$ that $a \lesssim b$ and $a \gtrsim b$ hold, where $a \lesssim b$ means that a can be bounded by a constant multiple of b uniformly in any parameters on which a, b may depend, and $a \gtrsim b$ means $b \lesssim a$. Since the V_j are not assumed to be subspaces of $H^k(\Omega)$, we have to be careful here, and define the energy norm for $u_j \in V_j$ in (2.2) by

$$\|u_j\|_{k,j}^2 := \|u_j\|_{L_2(\Omega)}^2 + \sum_{T \in \Delta_j} \|u_j\|_{H^k(T)}^2 .$$

In order to construct a multilevel splitting for the fine-scale subspace V_J, one needs suitable operators to project functions from the coarse-scale subspaces V_j ($j \le J$) into V_J. We introduce the linear prolongation operators

$$P_j \ : \ V_{j-1} \to V_j, \quad j = 1, \dots, J, \quad P_0 := 0, \tag{2.3}$$

and their iterates

$$\widetilde{P}_{j,J} := P_J P_{J-1} \cdots P_{j+1} \ : \ V_j \to V_J, \quad j = 0, \dots, J-1, \qquad \widetilde{P}_{J,J} := \mathrm{Id}\,. \tag{2.4}$$

We also need the L_2-orthogonal projection onto V_j,

$$Q_j : L_2(\Omega) \to V_j, \quad j = 0, \dots, J, \quad Q_{-1} := 0, \tag{2.5}$$

i.e., $(Q_j f, u_j) = (f, u_j)$ for all $u_j \in V_j$, with $f \in L_2(\Omega)$. Let $b_j(\cdot,\cdot) : \ V_j \times V_j \to R$ be another sequence of symmetric bilinear forms such that

$$b_j(u_j, u_j) \sim \rho^{2jk} \|u_j\|^2_{L_2}, \qquad u_j \in V_j. \tag{2.6}$$

For the following theorem, A_j, B_j denote the linear operators on V_j induced by the bilinear forms $a_j(\cdot,\cdot)$, $b_j(\cdot,\cdot)$, respectively.

Theorem 2.1. *The symmetric preconditioner C_J associated with the additive subspace splitting*

$$\{V_J; a_J(\cdot,\cdot)\} = \sum_{j=0}^{J} \widetilde{P}_{j,J} \{V_j; b_j(\cdot,\cdot)\} \tag{2.7}$$

and recursively given by

$$C_0 = B_0^{-1}, \qquad C_j = B_j^{-1} + P_j C_{j-1} P_j^T, \quad j = 1, \dots, J, \tag{2.8}$$

is optimal for preconditioning A_J; i.e.,

$$cond(C_J A_J) = \mathcal{O}(1), \qquad J \to \infty, \tag{2.9}$$

if and only if the two-sided inequality

$$\gamma |||u_J|||^2_{J,k} \le a_J(u_J, u_J) \le \Gamma |||u_J|||^2_{J,k}, \qquad u_J \in V_J, \tag{2.10}$$

holds with constants $0 < \gamma \le \Gamma < \infty$ independent of J. The norm $|||\cdot|||_{J,k}$ in (2.10) *is defined by*

$$|||u_J|||^2_{J,k} := \inf_{w_j \in V_j : \ u_J = \sum_{j=0}^J \widetilde{P}_{j,J} w_j} \sum_{j=0}^{J} \rho^{2jk} \|w_j\|^2_{L_2}. \tag{2.11}$$

More generally, the spectral condition number of $C_J A_J$ is exactly characterized by $cond(C_J A_J) = \inf(\Gamma/\gamma)$, where the infimum is with respect to the constants in (2.10).

This theorem clearly exhibits the role of the iterated prolongation operators $\widetilde{P}_{j,J}$ in establishing condition number bounds and makes precise the type of multilevel norms involved.

The present paper is about establishing the norm equivalence (2.10) for the sequence $\{S_j\}$ of linear finite element subspaces related to $\sqrt{3}$ refinement ($\rho = \sqrt{3}$), and the sequence $\{I_j\}$ of associated prolongation operators when applied to solving an $H^1_0(\Omega)$ elliptic problem ($k = 1$). Both S_j and I_j have been introduced in Section 1. We will make use of the simplifying property (1.3), and we put most of our effort in Section 3 into establishing

Proposition 2.2. *Suppose that $\mathbb{R}^2$ is equipped with a regular, quasiuniform triangulation Δ_0 with $h_0 \sim 1$, and suppose that the sequences $\{\Delta_j\}$, $\{S_j\}$, $\{I_j\}$ associated with $\sqrt{3}$ refinement are as described in Section 1. Then for the nested subsequence $\{S_{2j}\}$ we have the norm equivalence*

$$\|u_{2J}\|_{H^1}^2 \sim |||u_{2J}|||_1^2 := \inf_{w_{2j}\in S_{2j}:\ u_{2J}=\sum_{j=0}^J \widetilde{I}_{2j,2J} w_{2j}} \sum_{j=0}^J 3^{2j}\|w_{2j}\|_{L_2}^2. \tag{2.12}$$

The continuous analog of (2.12) *for $J \to \infty$ holds as well.*

A similar norm equivalence, with $I_{2j+2}I_{2j+1}$ replaced by the natural injection operators for $S_{2j} \subset S_{2j+2}$, is a well-known fact about approximation spaces related to linear finite element spaces on sequences of nested quasi-uniform triangulations (see Theorem 15 of [14]), and we will make use of it and its counterpart for $H^s(\mathbb{R}^2)$, $0 < s < 3/2$, when proving upper and lower bounds in (2.12). In particular, significant effort goes into the proof of a Bernstein-type estimate for $\widetilde{I}_{2j,2J}u_{2j}$ to hold in $H^s(\mathbb{R}^2)$ for some $1 < s < 3/2$.

The analog of Proposition 2.2 for general domains Ω and the whole ladder $\{S_j\}$ of linear finite element subspaces of $H_0^1(\Omega)$ will be proved in subsection 3.3. Although the proof is only a slight extension of the argument for Proposition 2.2, we have decided to separately deal with $\Omega = \mathbb{R}^2$ to more clearly exhibit the arguments needed.

3. Multilevel norm equivalences for $\sqrt{3}$ refinement

3.1. **Lower bounds: Jackson-type estimates.** Our aim is to establish the lower bound

$$|||u_{2J}|||_1^2 \lesssim \|u_{2J}\|_{H^1}^2, \qquad u_{2J} \in S_{2J}, \tag{3.1}$$

under the conditions of Proposition 2.2, i.e., for $\Omega = \mathbb{R}^2$.

We will depart from the previously mentioned standard norm equivalence

$$\|u_{2J}\|_{H^s(\Omega)}^2 \sim \inf_{w_{2j}\in S_{2j}:\ u_{2J}=\sum_{j=0}^J w_{2j}} \sum_{j=0}^J 3^{2js}\|w_{2j}\|_{L_2}^2, \qquad u_{2J} \in S_{2J}, \tag{3.2}$$

which holds for any $0 < s < 3/2$, with constants independent of u_{2J} and $J \geq 0$. This result holds also for the triadic refinement of an arbitrary polygonal domain $\Omega \subset \mathbb{R}^2$ satisfying the exterior cone condition (this excludes polygonal domains with slits) equipped with a regular, quasi-uniform triangulation Δ_0 of typical element diameter $h_0 \sim 1$ (see Theorem 15 in [14]). In this subsection, we use it with $s = 1$ only.

Choosing in (3.2) appropriate w_{2j} (e.g., $w_{2j} = Q_{2j}u_{2J} - Q_{2j-2}u_{2J}$, $j \geq 1$, and $w_0 = Q_0 u_{2J}$ will do) and setting $v_{2j} = w_0 + w_2 + \ldots + w_{2j} \in S_{2j}$ such that $u_{2J} = v_{2J}$, we have

$$\sum_{j=0}^J 3^{2j}\|w_{2j}\|_{L_2}^2 \lesssim \|u_{2J}\|_{H^1}^2. \tag{3.3}$$

Now define the decomposition

$$u_{2J} = \widetilde{I}_{0,2J} v_0 + \sum_{j=1}^{J} (\widetilde{I}_{2j,2J} v_{2j} - \widetilde{I}_{2j-2,2J} v_{2j-2})$$
$$= \widetilde{I}_{0,2J} w_0 + \sum_{j=1}^{J} \widetilde{I}_{2j,2J} (v_{2j} - I_{2j} I_{2j-1} v_{2j-2}),$$

and write

$$|||u_{2J}|||_1^2 \leq \|w_0\|_{L_2}^2 + \sum_{j=1}^{J} 3^{2j} \|v_{2j} - I_{2j} I_{2j-1} v_{2j-2}\|_{L_2}^2$$
$$\lesssim \sum_{j=0}^{J} 3^{2j} \|w_{2j}\|_{L_2}^2 + \sum_{j=0}^{J-1} 3^{2j} \| \underbrace{v_{2j} - I_{2j+2} I_{2j+1} v_{2j}}_{\hat{w}_{2j+2} :=} \|_{L_2}^2.$$

Since the first sum in the last expression can be estimated by (3.3), it remains to estimate the L_2-norms of $\hat{w}_{2j+2} \in S_{2j+2}$. This step corresponds to establishing an appropriate Jackson-type estimate for the given set of prolongation operators. The technical difficulty we have to overcome is that the prolongations I_{2j} do not preserve linear functions locally (unless Δ_0 is a uniform type-I triangulation). Using only the obvious fact that the prolongations locally reproduce constant functions will unfortunately not lead to the desired sharp bound (3.1); compare Remark 3.1 at the end of this subsection.

Due to the definition of the refinement process and of the prolongations I_{2j+1}, resp. I_{2j+2}, the only vertices of the triangulation Δ_{2j+2}, where $\hat{w}_{2j+2}$ does not vanish, are the vertices $P_{e,\pm}$ inserted in the even refinement step into edges from Δ_{2j}. More precisely, for each edge e from Δ_{2j} we have

$$\hat{w}_{2j+2}(P_{e,\pm}) = \pm \frac{\delta_e(v_{2j})}{9}, \qquad \delta_e(v_{2j}) := v_{2j}(P_+) + v_{2j}(P_-) - v_{2j}(Q_-) - v_{2j}(Q_+).$$

Here, $P_\pm$ are the endpoints of e, $Q_\pm$ denote the remaining vertices of the two triangles $T_{e,\pm}$ attached to e, and $P_{e,-} = (2P_- + P_+)/3$, $P_{e,+} = (P_- + 2P_+)/3$, consistent with the notation used before. Indeed, according to the definition of the prolongations via averaging (1.4), we have

$$I_{2j+2} I_{2j+1} v_{2j}(P_{e,-}) = \frac{1}{3} \Bigg(v_{2j}(P_-) + \frac{v_{2j}(P_-) + v_{2j}(P_+) + v_{2j}(Q_-)}{3} + \frac{v_{2j}(P_-) + v_{2j}(P_+) + v_{2j}(Q_+)}{3} \Bigg)$$
$$= \frac{5 v_{2j}(P_-) + 2 v_{2j}(P_+) + v_{2j}(Q_-) + v_{2j}(Q_+)}{9},$$

while $v_{2j}(P_{e,-}) = (2v_{2j}(P_-) + v_{2j}(P_+))/3$, and similarily for $P_{e,+}$. Thus,

$$\|\hat{w}_{2j+2}\|_{L_2}^2 \lesssim 3^{-2j} \sum_e \delta_e^2(v_{2j}) = \sum_{e'} 3^{-2j} \sum_{e \subset \Delta_{e'}:\, e \| e'} \delta_e(v_{2j})^2 \equiv \sum_{e'} S_{e'}, \tag{3.4}$$

where the summation in the first expression is with respect to all edges e in Δ_{2j}, while in the second expression the outer summation is with respect to all edges e' from the coarsest triangulation Δ_0, and the inner summation combines all edges e from Δ_{2j} that are parallel to e', and belong to the union $\Omega_{e'} := T_{e',-} \cup T_{e',+}$ of the

two coarse triangles attached to e'. Evidently, each e is accounted for in exactly one such inner summation term $S_{e'}$. To estimate $S_{e'}$, we map the region $\Omega_{e'}$ by a piecewise affine map $\phi_{e'}$ onto the unit square $Q = [0,1]^2$ subdivided into two triangles. Consider the function $\tilde{v}_{2j} := v_{2j} \circ \phi_{e'}^{-1}$, which is a linear finite element function on a uniform type-I triangulation of the unit square Q (with mesh-size 3^{-j}). It is not hard to see that

$$S_{e'} \lesssim \omega_2(3^{-j}, \tilde{v}_{2j})^2_{L_2(Q)} \lesssim \omega_2(3^{-j}, \tilde{u}_{2J})^2_{L_2(Q)} + \left(\sum_{\ell=j}^{J-1} \|w_{2\ell+2}\|_{L_2(\Omega_{e'})} \right)^2,$$

with a constant C independent of e' and v_{2j}. The first step is elementary (just observe that, for the edges e from Δ_{2j} under consideration for the sum $S_{e'}$, the expression $\delta_e(v_{2j})$ is bounded by the second difference of $\Delta_h^2 \tilde{v}_{2j}$ with step-size $|h| = 3^{-(j+1)}$ in the direction orthogonal to the image $\phi_{e'}(e)$ of e in Q on a sufficiently large subregion of $\phi_{e'}(\Omega_{e'})$); the second step uses standard properties of the L_2-modulus of continuity $\omega_2(t,f)_{L_2}$ applied to the decomposition

$$\tilde{v}_{2j} = \tilde{u}_{2J} - \sum_{\ell=j}^{J-1} (\tilde{v}_{2\ell+2} - \tilde{v}_{2\ell}),$$

together with the obvious fact that

$$\|\tilde{v}_{2\ell+2} - \tilde{v}_{2\ell}\|^2_{L_2(Q)} \sim \|w_{2\ell+2}\|^2_{L_2(\Omega_{e'})}.$$

Substituting this into (3.4), we get the desired estimate for the second sum in the expression for the upper bound for $|||u_{2J}|||_1^2$ as follows:

$$\begin{aligned}
\sum_{j=0}^{J-1} 3^{2j} \|\hat{w}_{2j+2}\|^2_{L_2} &\lesssim \sum_{e'} \left(\sum_{j=0}^{J-1} 3^{2j} \omega_2(3^{-j}, \tilde{u}_{2J})^2_{L_2(Q)} \right. \\
&\qquad \left. + \sum_{j=0}^{J-1} 3^{2j} \sum_{\ell=j}^{J-1} 3^{(\ell-j)} \|w_{2\ell+2}\|^2_{L_2(\Omega_{e'})} \right) \\
&\lesssim \sum_{e'} \|\tilde{u}_{2J}\|^2_{H^1(Q)} + \sum_{j=0}^{J-1} 3^{2j} \sum_{e'} \|w_{2j+2}\|^2_{L_2(\Omega_{e'})} \\
&\lesssim \sum_{e'} \|u_{2J}\|^2_{H^1(\Omega_{e'})} + \sum_{j=0}^{J-1} 3^{2j} \|w_{2j+2}\|^2_{L_2} \lesssim \|u_{2J}\|^2_{H^1}.
\end{aligned}$$

Here we used that

$$\begin{aligned}
\Big(\sum_{\ell=j}^{J-1} \|w_{2\ell+2}\|_{L_2(\Omega_{e'})}\Big)^2 &\le \Big(\sum_{\ell=j}^{J-1} 3^{j-\ell}\Big) \cdot \Big(\sum_{\ell=j}^{J-1} 3^{\ell-j} \|w_{2\ell+2}\|^2_{L_2(\Omega_{e'})}\Big) \\
&\lesssim \sum_{\ell=j}^{J-1} 3^{\ell-j} \|w_{2\ell+2}\|^2_{L_2(\Omega_{e'})}.
\end{aligned}$$

The term involving the moduli of smoothness of $\tilde{u}_{2J} = u_{2J} \circ \phi_{e'}^{-1}$ was estimated by the square of the norm of $\tilde{u}_{2J}$ in the Besov space $B^1_{2,2}(Q)$, which is equivalent to its

norm in $H^1(Q)$. Furthermore, we used that the considered piecewise affine transformations $\phi_{e'}$, resp. $\phi_{e'}^{-1}$, are linear homomorphisms between the corresponding H^1 spaces, and that

$$\|f\|_{L_2}^2 = \frac{1}{3}\sum_{e'} \|f\|_{L_2(\Omega_{e'})}^2, \qquad \|f\|_{H^1}^2 = \frac{1}{3}\sum_{e'} \|f\|_{H^1(\Omega_{e'})}^2$$

for any $f \in H^1$ by the additivity of the involved norms with respect to triangular partitions of the underlying domains. Altogether, this establishes the desired lower bound (3.1).

Remark 3.1. Using the fact that the L_2 orthogonal projections Q_j are H^1-stable on regular, quasi-uniform meshes, i.e.,

$$\|Q_j u\|_{H^1} \lesssim \|u\|_{H^1},$$

see, e.g., [3], one can easily prove a suboptimal lower bound (involving an additional factor J). Indeed, an estimate for the L_2-norm of $\hat{w}_{2j+2}$ is obtained by using the fact that the prolongations I_j locally reproduce constant functions

$$\|v_{2j} - I_{2j+2}I_{2j+1}v_{2j}\|_{L_2}^2 \lesssim 3^{-2j}\|v_{2j}\|_{H^1}^2,$$

which combined with

$$\|v_{2j}\|_{H^1}^2 = \|Q_{2j}u_{2J}\|_{H^1}^2 \lesssim \|u_{2J}\|_{H^1}^2$$

yields the suboptimal bound $\lesssim J\|u_{2J}\|_{H^1}^2$ for the second sum.

This simplified argument also goes through for the general case considered in Section 3.3 below; however, it does not lead to the best possible estimate. It is also not clear at the moment whether the main multilevel norm equivalence proved later in this paper in Theorem 3.5 will imply the H^1-stability of the L_2-orthogonal projections $\widetilde{Q}_{j,J}$ onto the subspaces $\widetilde{S}_{j,J} := \widetilde{I}_{j,J}S_j$, $j < J$; see [1, Section 9] for the argument in the nested case. H^1-stability of $\widetilde{Q}_{j,J}$ would be useful as a tool in the analysis of an adaptive version of the proposed $\sqrt{3}$ preconditioning. Note that $\{\widetilde{S}_{j,J}\}_{j=0,\dots,J}$ is the nested multilevel sequence of subspaces of S_J that the iterated prolongation operators $\widetilde{I}_{j,J}$ generate from the original nonnested ladder $\{S_j\}_{j=0,\dots,J}$.

3.2. **Upper bounds: Bernstein-type estimates.** In this section we establish the following Bernstein-type estimate for the spaces $\widetilde{I}_{2j,2J}S_{2j}$:

Theorem 3.2. *Let Δ_0 be a regular, quasi-uniform triangulation of $\mathbb{R}^2$ ($h_0 \sim 1$), and let $\{\Delta_j\}$ be obtained by $\sqrt{3}$ refinement, as specified above. Then the iterated prolongation operators satisfy*

$$\|\widetilde{I}_{2j,2J}v_{2j}\|_{H^s} \lesssim 3^{js}\|v_{2j}\|_{L_2}, \qquad v_{2j} \in S_{2j}, \quad 0 \le j \le J < \infty, \tag{3.5}$$

for the range $0 < s < s_0$, where $s_0 := 1 + \log_3(9/5)/2 > 1$, with constants independent of v_{2j}, j, and J.

Proof. For the proof we again rely on the norm equivalence (3.2). A simple consequence is that if we denote $v_{2m} = I_{2m}I_{2m-1}\cdots I_{2j+1}v_{2j}$ and $w_{2m+2} = v_{2m+2} - v_{2m}$, then

$$\|\widetilde{I}_{2j,2J}v_{2j}\|_{H^s}^2 \lesssim 3^{2js}\|v_{2j}\|_{L_2}^2 + \sum_{m=j}^{J-1} 3^{2ms}\|w_{2m+2}\|_{L_2}^2. \tag{3.6}$$

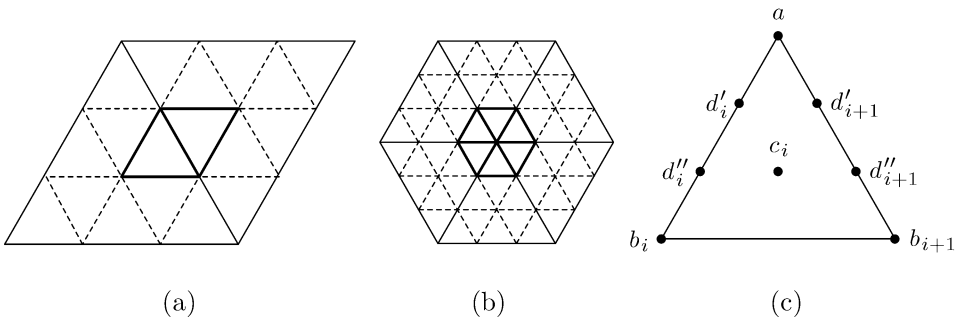

FIGURE 4. (a) E'_e: Group of 5 edges in Δ_{2m+2} associated with edge e in Δ_{2m}. (b) E'_P: Group of $2K_P$ edges in Δ_{2m+2} associated with vertex P from Δ_{2m}. (c) Notation for the nodal values of v_{2m} and v_{2m+2} for triangle PP_iP_{i+1} near vertex P.

It is obvious that $\|w_{2m+2}\|^2_{L_2} \lesssim \|v_{2m}\|^2_{L_2}$ by the L_2-boundedness of the prolongation operators. The main observation for the proof of (3.5) is that the L_2-norms of w_{2m+2} decay at a geometric rate:

$$\|w_{2m+2}\|^2_{L_2} \lesssim 3^{-2(m-j)s_0}\|v_{2j}\|^2_{L_2}, \qquad m \geq j, \tag{3.7}$$

with the above defined $s_0 > 1$.

The proof of (3.7) is tedious but elementary. First observe that by construction we have

$$\|w_{2m+2}\|^2_{L_2} \sim 3^{-2m}\sum_e \delta_e(v_{2m})^2 \equiv 3^{-2m}\Sigma_m, \qquad m \geq j, \tag{3.8}$$

where the summation is with respect to the edges e of Δ_{2m}, and the differences

$$\delta_e(v_{2m}) = v_{2m}(P_+) + v_{2m}(P_-) - v_{2m}(Q_-) - v_{2m}(Q_+)$$

mimic the mixed second derivative of v near e. For the notation and some calculations leading to this result, see the previous subsection.

We are going to prove a recursive estimate for Σ_m. For further use, note that

$$\Sigma_m = \frac{1}{2}\sum_P \delta_P(v_{2m})^2, \qquad \delta_P(v_{2m}) := \sum_{e:P\in\bar{e}} \delta_e(v_{2m})^2, \tag{3.9}$$

where the summation is now over all vertices P of Δ_{2m}. One easily checks that

$$\Sigma_{m+1} = \sum_e \sum_{e'\in E'_e} \delta_{e'}(v_{2m+2})^2 + \sum_P \sum_{e'\in E'_P} \delta_{e'}(v_{2m+2})^2,$$

where the outer summations are with respect to edges e and vertices P of Δ_{2m} (not Δ_{2m+2}) while for the inner summations E'_e denotes a group of 5 edges in Δ_{2m+2} associated with e as shown in Figure 4(a), and E'_P denotes the group of $2K_P$ edges in Δ_{2m+2} associated with a coarse vertex P as shown in Figure 4(b). Here K_P denotes the valence of P.

For evaluating $\delta_{e'}(v_{2m+2})^2$, consider the 1-ring of triangles in Δ_{2m} attached to P, and denote by $e_1, e_2, \ldots, e_{K_P}$ the edges in Δ_{2m} emanating from P (ordered counterclockwise). Figure 4(c) shows the chosen notation for the nodal values (denoted by $a = v_{2m}(P)$ and $b_i = v_{2m}(P_i)$, $i = 1, \ldots, K_P$) of v_{2m} near P, and the

computed nodal values of $v_{2m+2} = I_{2m+2}I_{2m+1}v_{2m}$ at the barycenters M_i of the triangle PP_iP_{i+1},

$$c_i = v_{2m}(M_i) = \frac{v_{2m}(P) + v_{2m}(P_i) + v_{2m}(P_{i+1})}{3} = \frac{3a + 3b_i + 3b_{i+1}}{9},$$

and at the newly inserted points $P_i' = (2P + P_i)/3$ and $P_i'' = (P + 2P_i)/3$ on the edges $e_i = PP_i$ of Δ_{2m}:

$$\begin{aligned} d_i' &= \frac{v_{2m}(P) + v_{2m}(M_i) + v_{2m}(M_{i-1})}{3} = \frac{5a + b_{i-1} + 2b_i + b_{i+1}}{9}, \\ d_i'' &= \frac{v_{2m}(P_i) + v_{2m}(M_i) + v_{2m}(M_{i-1})}{3} = \frac{2a + b_{i-1} + 5b_i + b_{i+1}}{9}. \end{aligned}$$

Using the nodal values of v_{2m+2} derived before, one can easily compute that

$$\delta_{e'}(v_{2m+2})^2 = \delta_{e_i}(v_{2m})^2/81, \qquad e' \in E'_{e_i}, \quad i = 1, \dots, 6.$$

This implies

$$\sum_e \sum_{e' \in E'_e} \delta_{e'}(v_{2m+2})^2 = 5\Sigma_m/81. \tag{3.10}$$

For the two types of edges in E'_P, we have the following. For $e' = PP_i'$ on e_i we have

$$\begin{aligned} \delta_{e'}(v_{2m+2}) &= \frac{4a - b_{i-2} - b_{i-1} - b_{i+1} - b_{i+2}}{9} \\ &= \frac{\delta_{e_{i-1}}(v_{2m}) + 2\delta_{e_i}(v_{2m}) + \delta_{e_{i+1}}(v_{2m})}{9}. \end{aligned}$$

Similarly, for $e' = P_i'P_{i+1}'$ connecting e_i and e_{i+1}, we have

$$\delta_{e'}(v_{2m+2}) = \frac{b_{i-1} + b_{i+2} - 2a}{9} = -\frac{\delta_{e_i}(v_{2m}) + \delta_{e_{i+1}}(v_{2m})}{9}.$$

Thus, we get

$$\begin{aligned} &\sum_P \sum_{e' \in E'_P} \delta_{e'}(v_{2m+2})^2 \\ &\quad = \sum_P \sum_{i=1}^{K_P} \frac{(\delta_{e_{i-1}}(v_{2m}) + 2\delta_{e_i}(v_{2m}) + \delta_{e_{i+1}}(v_{2m}))^2 + (\delta_{e_i}(v_{2m}) + \delta_{e_{i+1}}(v_{2m}))^2}{81} \\ &\quad \le \frac{20}{81} \sum_P \sum_{i=1}^{K_P} \delta_{e_i}(v_{2m})^2 = \frac{40}{81}\Sigma_m. \end{aligned}$$

Substituting this together with (3.10) into (3.9) we see that

$$\Sigma_{m+1} \le \frac{5}{9}\Sigma_m, \qquad m \ge j. \tag{3.11}$$

Further substitution into (3.8) yields

$$\|w_{2m+2}\|_{L_2}^2 \lesssim 3^{-2m}\Sigma_m \lesssim 3^{-2(m-j)}(5/9)^{m-j}3^{-2j}\Sigma_j \lesssim (5/81)^{m-j}\,\|v_{2j}\|_{L_2}^2.$$

This is the desired estimate (3.7). Substitution of the latter into (3.6) yields (3.5) for $0 < s < s_0$:

$$\left\|\widetilde{I}_{2j,2J}v_{2j}\right\|_{H^s}^2 \lesssim 3^{2js}\,\|v_{2j}\|_{L_2}^2 \left(1 + \sum_{m=j}^{J-1} 3^{2(j-m)(s_0-s)}\right) \lesssim 3^{2js}\,\|v_{2j}\|_{L_2}^2. \qquad \square$$

With the Bernstein-type estimate of Theorem 3.2 established, the upper bound of the norm equivalence stated in Proposition 2.2 follows by a standard argument: Fix $\epsilon \in (0,1)$ such that $1+\epsilon < s_0$, and consider an arbitrary decomposition

$$u_{2J} = \sum_{j=0}^{J} \widetilde{I}_{2j,2J} w_{2j}, \qquad w_{2j} \in S_{2j}.$$

Then, using well-known properties of the Hilbert spaces $H^1(\mathbb{R}^2)$ and $H^{1\pm\epsilon}(\mathbb{R}^2)$, we have

$$\begin{aligned}
\|u_{2J}\|_{H^1}^2 &= (\sum_{j=0}^{J} \widetilde{I}_{2j,2J} w_{2j}, \sum_{j=0}^{J} \widetilde{I}_{2j,2J} w_{2j})_{H^1} \\
&\le 2 \sum_{j=0}^{J} \sum_{\ell=j}^{J} \left| (\widetilde{I}_{2j,2J} w_{2j}, \widetilde{I}_{2\ell,2J} w_{2\ell})_{H^1} \right| \\
&\lesssim \sum_{j=0}^{J} \sum_{\ell=j}^{J} \|\widetilde{I}_{2j,2J} w_{2j}\|_{H^{1+\epsilon}} \|\widetilde{I}_{2\ell,2J} w_{2\ell}\|_{H^{1-\epsilon}} \\
&\lesssim \sum_{j=0}^{J} \sum_{\ell=j}^{J} 3^{\epsilon(j-\ell)} (3^j \|w_{2j})\|_{L_2}) (3^\ell \|w_{2\ell}\|_{L_2}) \lesssim \sum_{j=0}^{J} 3^{2j} \|w_{2j}\|_{L_2}^2.
\end{aligned}$$

It remains to take the infimum with respect to all admissible decompositions of u_{2J}.

Remark 3.3. If we establish the Bernstein estimate (3.5) only in the case $s = 1$ (this is what has usually been done in previous investigations for nonnested finite element discretizations), we can still prove the suboptimal bound

$$\|u_{2J}\|_{H^1}^2 \lesssim J |||u_{2J}|||_1^2.$$

This follows immediately from

$$\|u_{2J}\|_{H^1}^2 \le \left(\sum_{j=0}^{J} \left\| \widetilde{I}_{2j,2J} w_{2j} \right\|_{H^1} \right)^2 \le J \sum_{j=0}^{J} \left\| \widetilde{I}_{2j,2J} w_{2j} \right\|_{H^1}^2 \lesssim J \sum_{j=0}^{J} 3^{2j} \|w_{2j}\|_{L_2}^2,$$

where the decomposition $u_{2J} = \sum_{j=0}^{J} \widetilde{I}_{2j,2J} w_{2j}$ was chosen arbitrarily.

Remark 3.4. If we let $J \to \infty$, then the above proof establishes de facto that the sequence $\{\widetilde{I}_{2j,2J} v_{2j},\ J \ge j\}$ converges in H^s for any $s < s_0$. The limit functions have thus a Sobolev smoothness exponent at least $s_0 = 1 + \log_3(9/5)/2 = 1.2675...$, independently of Δ_0. Figure 5 depicts the limit functions if we set $j = 0$ and choose as v_0 a nodal basis function from S_0 at vertices of valence 6 and 4.

For a more detailed account on the connection between the smoothness of limit functions for subdivision processes generated by prolongation operators used in multilevel preconditioners for symmetric H^1-elliptic problems, and the upper spectral bounds for the resulting multilevel preconditioner, we refer to a recent case study [17] for the nonconforming P1 element.

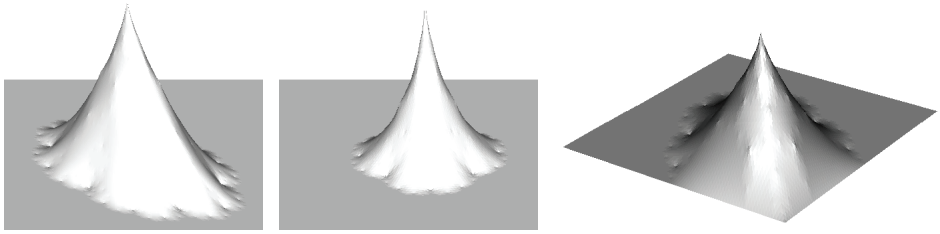

FIGURE 5. Examples of limit functions centered around vertices of different valence and near the Dirichlet boundary

3.3. **General case: Bounded domains and odd J.** So far we have only established the theoretical estimate of Proposition 2.2 for $\{S_{2j}\}$ and $\Omega = \mathbb{R}^2$. The extension to domains will be exemplified with an application to a symmetric $H_0^1(\Omega)$ elliptic boundary value problem in mind.

From now on, let Ω be a bounded polygonal domain satisfying the exterior cone condition, equipped with an appropriate Δ_0 such that $h_0 \sim 1$. The $\sqrt{3}$ refinement process as explained in Section 1 yields $\{\Delta_j\}$, the spaces S_j consist of all linear finite element functions on Δ_j that simultaneously belong to $H_0^1(\Omega)$, and the prolongations $I_j : S_{j-1} \to S_j$ are the same as in the $\mathbb{R}^2$ case but modified for new vertices at the boundary of Ω such that zero Dirichlet boundary conditions are automatically enforced.

Theorem 3.5. *Suppose the domain Ω and the sequences $\{\Delta_j\}$, $\{S_j\}$, $\{I_j\}$ are as described before. Then for the nonnested ladder $\{S_j\}$ we have the norm equivalence*

$$\|u_J\|^2_{H^1(\Omega)} \sim |||u_J|||^2_{J,1} := \inf_{w_j \in S_j:\ u_J = \sum_{j=0}^J \widetilde{I}_{j,J} w_j} \sum_{j=0}^J 3^j \|w_j\|^2_{L_2(\Omega)}, \tag{3.12}$$

with constants independent of $u_J \in S_J$ and $J \geq 0$.

Proof. First, the statement reduces to the following direct analog of Proposition 2.2:

$$\|u_{2J}\|^2_{H^1(\Omega)} \sim |||u_{2J}|||^2_1 := \inf_{w_{2j} \in S_{2j}:\ u_{2J} = \sum_{j=0}^J \widetilde{I}_{2j,2J} w_{2j}} \sum_{j=0}^J 3^{2j} \|w_{2j}\|^2_{L_2(\Omega)}. \tag{3.13}$$

Indeed, by the definition of the triple norms in (3.12) and (3.13), we obviously have $|||u_{2J}|||^2_{2J,1} \leq |||u_{2J}|||^2_1$. For the other direction, take any admissible decomposition

$$u_{2J} = \widetilde{I}_{0,2J} w_0 + \widetilde{I}_{1,2J} w_1 + \cdots + w_{2J},$$

and rewrite it in the form

$$u_{2J} = \widetilde{I}_{0,2J} w_0 + \widetilde{I}_{2,2J}(I_2 w_1 + w_2) + \cdots + (I_{2J} w_{2J-1} + w_{2J}).$$

Thus,

$$\begin{aligned}|||u_{2J}|||_1^2 &\leq \|w_0\|^2_{L_2(\Omega)} + \sum_{j=1}^{J} 3^{2j}\|I_{2j}w_{2j-1} + w_{2j}\|^2_{L_2(\Omega)} \\ &\lesssim \|w_0\|^2_{L_2(\Omega)} + \sum_{j=1}^{J} 3^{2j}(\|w_{2j-1}\|^2_{L_2(\Omega)} + \|w_{2j}\|^2_{L_2(\Omega)}) \lesssim \sum_{j=0}^{2J} 3^{2j}\|w_j\|^2_{L_2(\Omega)}.\end{aligned}$$

Besides the triangle inequality, we have used the uniform boundedness of the L_2 norm of $I_j : S_{j-1} \to S_j$. Taking the infimum with respect to all admissible decompositions, we get $|||u_{2J}|||_1^2 \lesssim |||u_{2J}|||^2_{2J,1}$.

For odd indices, the argument is as follows. Let $R_{2J} : S_{2J+1} \to S_{2J}$ be the restriction operator that interpolates u_{2J+1} at the vertices of Δ_{2J}. Set $\hat{u}_{2J} = R_{2J}u_{2J+1} \in S_{2J}$ and $w_{2J+1} := u_{2J+1} - I_{2J+1}\hat{u}_{2J} \in S_{2J+1}$. By looking at the nodal values of these two finite element functions, it is easy to see that

$$\|\hat{u}_{2J}\|^2_{H^1(\Omega)} \lesssim \|u_{2J+1}\|^2_{H^1(\Omega)}, \qquad 3^{2J+1}\|w_{2J+1}\|^2_{L_2(\Omega)} \lesssim \|u_{2J+1}\|^2_{H^1(\Omega)}.$$

Thus,

$$\begin{aligned}\|u_{2J+1}\|^2_{H^1(\Omega)} &\gtrsim \|\hat{u}_{2J}\|^2_{H^1(\Omega)} + 3^{2J+1}\|w_{2J+1}\|^2_{L_2(\Omega)} \\ &\gtrsim |||\hat{u}_{2J}|||^2_{2J,1} + 3^{2J+1}\|w_{2J+1}\|^2_{L_2(\Omega)} \gtrsim |||u_{2J+1}|||^2_{2J+1,1},\end{aligned}$$

since the admissible decomposition $\hat{u}_{2J} = \sum_{j=0}^{2J} \widetilde{I}_{j,2J}w_j$, for which

$$\|\hat{u}_{2J}\|^2_{H^1(\Omega)} \gtrsim |||\hat{u}_{2J}|||^2_{2J,1} \gtrsim \sum_{j=0}^{2J} 3^j\|w_j\|^2_{L_2(\Omega)}$$

due to the already established result for S_{2J}, automatically gives an admissible decomposition for u_{2J+1}:

$$u_{2J+1} = w_{2J+1} + I_{2J+1}\hat{u}_{2J} = w_{2J+1} + I_{2J+1}(\sum_{j=0}^{2J} \widetilde{I}_{j,2J}w_j) = \sum_{j=0}^{2J+1} \widetilde{I}_{j,2J+1}w_j.$$

In the opposite direction, start with an arbitrary decomposition

$$u_{2J+1} = \sum_{j=0}^{2J+1} \widetilde{I}_{j,2J+1}w_j \equiv w_{2J+1} + I_{2J+1}(\sum_{j=0}^{2J} w_j),$$

and use the boundedness of $I_{2J+1} : S_{2J} \to S_{2J+1}$ in the H^1 norm and the inverse inequality on S_{2J+1}:

$$\begin{aligned}\|u_{2J+1}\|^2_{H^1(\Omega)} &\leq 2\|I_{2J+1}(\sum_{j=0}^{2J} w_j)\|^2_{H^1(\Omega)} + \|w_{2J+1}\|^2_{H^1(\Omega)} \\ &\lesssim \|\sum_{j=0}^{2J} w_j\|^2_{H^1(\Omega)} + 3^{2J+1}\|w_{2J+1}\|^2_{L_2(\Omega)} \lesssim \sum_{j=0}^{2J+1} 3^j\|w_j\|^2_{L_2(\Omega)}.\end{aligned}$$

In the last step, we have used the already established inequality for even indices. Taking the infimum with respect to all decompositions, we finish the reduction step.

It remains to prove (3.13). This requires only minor changes compared to the proof given in subsections 3.1 and 3.2, which we now list. Note that the basic norm equivalence (3.2) holds also for the case that the definition of the ladder

$\{S_{2j}\}$ involves zero Dirichlet boundary conditions, however, with the restriction $1/2 < s < 3/2$; see [14, Theorem 18]. This is enough for the given application since for the lower bound (Section 3.1) we needed only $s = 1$, while the upper bound (Section 3.2) required values $s = 1, 1 \pm \epsilon$ with $0 < \epsilon < 1/2$, which is also covered. As in Section 3.1, the crucial step in the proof of the lower bound is the estimation of $\|\hat{w}_{2j+2}\|^2_{L_2(\Omega)}$, which is carried out using the bound (3.4). The only change in (3.4) is that the summation defining $S_{e'}$ for boundary edges in Δ_0 is only with respect to edges e parallel to e' and *interior* to the only triangle $T_{e',+} \equiv \Omega_{e'}$ from Δ_0 attached to e' (the outer summation has still to be carried out with respect to all edges e' of Δ_0; for interior e' the definition of $S_{e'}$ remains unchanged). The rest of the argument goes through as before, terms for boundary edges can directly be estimated by second order moduli of continuity, and there is no need in using piecewise affine maps.

We also claim that the statement of Theorem 3.2 carries over at least for $1/2 < s < s_0$. The crucial step is proving sufficient geometric decay for $\|w_{2m+2}\|^2_{L_2}$ or, what is the same, for Σ_m whose definition changes as follows: According to our boundary treatment the differences w_{2m+2} vanish identically on the boundary. Thus, (3.8) holds if the summation on the right is with respect to all interior edges e of Δ_{2m} only. This expression is again denoted by Σ_m.

With this at hand, the estimate $\Sigma_{m+1} \le (5/9)\Sigma_m$, $m < j$, will not change. Indeed, Σ_{m+1} can be split into a sum over edge groups E'_e associated with the interior edges of Δ_{2m} and edge groups E'_P associated with vertices of Δ_{2m}. The latter are modified for P on the boundary: Let $e_0, \dots, e_{K_P}$ denote the edges emanating from such a P, starting from the boundary edge e_0 in the counterclockwise direction and ending in another boundary edge e_{K_P}. Then by construction, $\delta_{e_0}(v_{2m}) = \delta_{e_{K_P}}(v_{2m}) = 0$, and

$$\delta_P(v_{2m})^2 := \sum_{i=1}^{K_P-1} \delta_{e_i}(v_{2m})^2 = \sum_{i=0}^{K_P} \delta_{e_i}(v_{2m})^2.$$

All formulas remain valid; in particular, for edges $e' \in E'_{e_0}$ interior to Δ_{2m+2}, we automatically have $\delta_{e'}(v_{2m+2})^2 = \delta_{e_0}(v_{2m})^2/81 = 0$, while the expressions for edges $e' \in E'_P$ interior to Δ_{2m+2} close to e_0 simplify to $(2\delta_{e_1}(v_{2m}) + \delta_{e_2}(v_{2m+1}))^2/81$, resp. $\delta_{e_1}(v_{2m})^2/81$, and similarly for the edges e' close to e_{K_P}. Thus, the geometric decay of $\{\Sigma_m\}$ (with rate $5/9$) follows by the same estimation steps. All other arguments are the same for domains (with the extension property for Sobolev spaces) and $\mathbb{R}^2$. The visualization of the limit behavior of the prolongation process for $J \to \infty$ provided in Figure 5 c) confirms this. This concludes the proof of Theorem 3.5. □

Remark 3.6. Although we have only dealt with the case of homogeneous Dirichlet boundary conditions, it is possible to get optimality results for Neumann and Robin boundary conditions and their combinations as well (under the assumption that the type of boundary condition does not change inside any boundary edge of Δ_0). The treatment of the boundary modifications can be based on the observation that the definition of I_{2j} at newly inserted boundary vertices (by linear interpolation along the boundary edge) can be achieved if we solely use the averaging rule (1.4), after extending functions from S_{2j-2} to the virtual boundary triangles as shown in Figure 6. This extension trick allows us to derive estimates in the case of polygonal domains Ω by basically reducing them to the $\mathbb{R}^2$ case since the special boundary

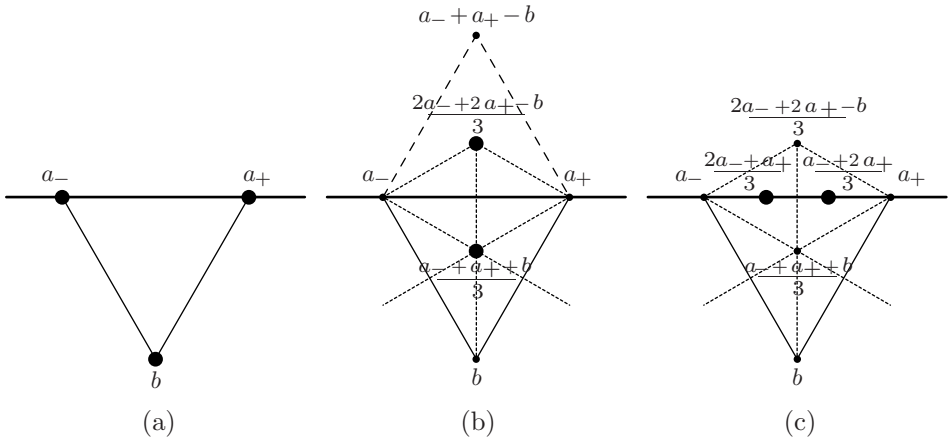

FIGURE 6. (a) Function values near the boundary. (b) Function values after one step of $\sqrt{3}$ refinement. We introduce a virtual triangle to compute the function value outside the domain. (c) The function values that are computed on the boundary after the second step of $\sqrt{3}$ refinement preserve linear functions on the boundary.

rules for prolongations appear now as normal averaging rules for the extension (whose H^1 and L_2 norms are easily controlled).

4. An optimal BPX-type preconditioner

In this section we provide some numerical evidence concerning the preconditioning performance of BPX-type multilevel solvers for $\sqrt{3}$ refinement covered by our theoretical optimality result (Theorem 3.5, in conjunction with Theorem 2.1). Details will be given for the variational Poisson problem (2.1), where $a_j(\cdot,\cdot)$ is the symmetric, continuous, and coercive bilinear form induced by (1.1), given by the restriction of $a(u,v) \equiv (\nabla u, \nabla v)_{L_2(\Omega)}$ to S_j, and $(\cdot,\cdot)_{L_2(\Omega)}$ denotes the $L_2(\Omega)$ scalar product. If we combine Theorem 2.1 and Theorem 3.5, we have so far established that the space splitting

$$\{S_J; a(\cdot,\cdot)\} = \sum_{j=0}^{J} \widetilde{I}_{j,J} \left\{ S_j; 3^j (\cdot,\cdot)_{L_2(\Omega)} \right\} \tag{4.1}$$

leads to an asymptotically optimal preconditioner for the Galerkin discretization of the Poisson problem on S_J. It is customary to replace the auxiliary bilinear forms $b_j(u_j, v_j) = 3^j (u_j, v_j)_{L_2(\Omega)}$ appearing in (4.1) by spectrally equivalent forms that lead to even simpler operations B_j^{-1} if implemented in the standard finite element nodal bases in S_j.

BPX-type multilevel solvers are characterized by *diagonal* matrices B_j and B_j^{-1}. E.g., we could use the L_2-stability of the nodal bases $\Phi_j := \{\phi_{j,P}\}$ in S_j, which can be written in the form

$$3^j \| \sum_P c_{j,P} \phi_{j,P} \|^2_{L_2(\Omega)} \sim \sum_P c^2_{j,P} \sim \sum_P c^2_{j,P} a(\phi_{j,P}, \phi_{j,P}). \tag{4.2}$$

Here summation is with respect to all interior vertices P in Δ_j, and constants are independent of $\{c_{j,P}\}$ and j. If we choose one of the latter two expressions (representing the squares of certain ℓ_2 coefficient norms on S_j), the resulting auxiliary $b_j(\cdot,\cdot)$ lead to $B_j = \mathrm{Id}_j$, resp. $B_j = \mathrm{diag}(a(\phi_{j,P}, \phi_{j,P}))$, and are easy to implement.

Another natural version of a BPX-type preconditioner results from a reinterpretation of the additive space splitting (4.1) in terms of *frames*. Substituting the first part of (4.2) into the norm equivalence of Theorem 3.5, we have

$$\|u_J\|^2_{H^1(\Omega)} \sim \inf_{u_J=\sum_{j=0}^J \sum_P c_{j,P}\widetilde{I}_{j,J}\phi_{j,P}} \sum_{j=0}^J \sum_P c^2_{j,P}, \qquad u_J \in S_J. \tag{4.3}$$

This means that the redundant system $\bigcup_{j=0}^J \widetilde{I}_{j,J}\Phi_j$ is a frame in the finite-dimensional space S_J equipped with the Hilbert space structure inherited from $H^1(\Omega)$, resp. from the bilinear form $a(\cdot,\cdot)$, with frame bounds independent of J. Moreover, this frame generates an asymptotically optimal preconditioning method (with B_j the identity operator). These properties do not change if we rescale the functions $\tilde\phi_{j,P} := \widetilde{I}_{j,J}\phi_{j,P} \in S_J$ to $d^{-1}_{j,P}\tilde\phi_{j,P}$ with constants $d_{j,P} \sim 1$. Popular choices are

$$d^{(1)}_{j,P} = 3^{j/2}\|\tilde\phi_{j,P}\|_{L_2(\Omega)}$$

or

$$d^{(2)}_{j,P} = \sqrt{a(\tilde\phi_{j,P}, \tilde\phi_{j,P})}. \tag{4.4}$$

Given that $d^{(1)}_{j,P} \sim d^{(2)}_{j,P} \sim 1$ has been validated numerically, a formal proof is left as an exercise to the reader. We note that the recursive implementation of the preconditioner corresponding to these frames can be recovered from Theorem 2.1 by setting $P_j = I_j$ and $B_j = \mathrm{diag}(\{d^{(2)}_{j,P}\})$. In the tests below, we have used both the standard BPX, where $d_{j,P} = 1$, and the so-called multilevel diagonal scaling version of BPX (for short MDS-BPX), where $d_{j,P} = d^{(2)}_{j,P}$ is given by (4.4).

We can also define the corresponding hierarchical basis (HB) preconditioners by reducing the number of functions in the above frame systems: We only take those $\tilde\phi_{j,P}$ corresponding to the *newly created* interior vertices in Δ_j. It can be shown using standard techniques combined with the properties that we derived for the BPX-type preconditioners that such an HB system is indeed a basis in S_J, and leads to a preconditioner C_J with condition number bounds of the order $\mathrm{cond}(C_J A_J) = \mathcal{O}(J^2)$, which is similar to Yserentant's result in [18].

We conclude this section by presenting some numerical tests. We solve the Poisson problem (1.1) on the unit square, where we choose the initial triangulation Δ_0 as indicated in Figure 7, and where f is such that the exact solution u is given by $x(1-x)y(1-y)$. The starting vector for each iteration is $\mathbf{u}^{(0)}_J = 0$. We stop the conjugate gradient iteration if the H^1-norm of the residual is proportional to the a priori bound for the discretization error, i.e., if

$$\|r_J\|_{H^1} \le \epsilon_0 h.$$

Table 1 and Table 2 show the results for a regular, resp. irregular, triangulation Δ_0 with $\epsilon_0 = 0.01$. Both tables have the same structure. The first column contains the maximum resolution level J. Then we distinguish between the results for the BPX preconditioner based on linear averaging $\sqrt{3}$ subdivision and the results for the classical BPX preconditioner from [4]. For each preconditioner we display the size of the underlying frame system denoted by dim, an estimate of the spectral

condition number κ of the system matrix for the linear system of equations that is solved, the H^1-norm of the residuals corresponding to the approximate solution, and the number of iterations that are needed to reach discretization error accuracy.

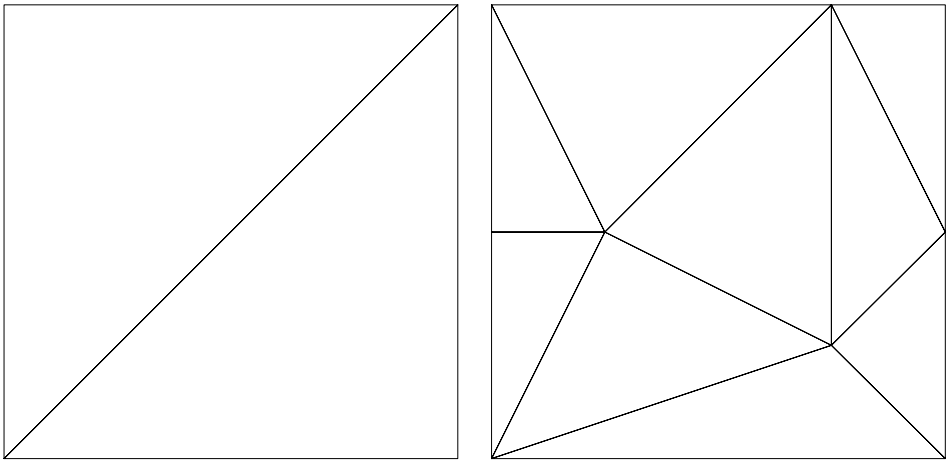

(a) regular triangulation (b) irregular triangulation

FIGURE 7. Initial triangulations Δ_0 used in the numerical tests

TABLE 1. Iteration history for the Poisson problem where Δ_0 is as in Figure 7 (a). We compare the linear averaging $\sqrt{3}$ subdivision BPX preconditioner with the classical BPX preconditioner.

	$\sqrt{3}$				dyadic			
J	dim	κ	residual	#iter	dim	κ	residual	#iter
3	28	3.91	1.59e-3	5	59	5.31	7.56e-4	7
4	92	6.32	4.43e-4	7	284	7.06	6.036e-4	9
5	318	7.32	2.85e-4	8	1245	8.27	2.58e-4	11
6	994	8.39	2.04e-4	9	5214	9.22	1.10e-4	13
7	3128	8.90	1.12e-4	10	21343	9.99	4.54e-5	15
8	9528	9.53	5.40e-5	11	86368	10.64	3.49e-5	16
9	29050	9.81	2.92e-5	12	–	–	–	–
10	87614	10.25	3.02e-5	12	–	–	–	–

The remaining Tables 3 and 4 show the results for the BPX-MDS preconditioner and, for comparison, for the suboptimal HB-MDS preconditioner. Note that multilevel diagonal scaling leads to slight improvements, and that (as expected) the hierarchical basis preconditioner needs generally more iterations to reach the target accuracy. The reported cpu times are only of relative value (the C++ implementation used was run on a laptop with an Intel Pentium M 2 GHz processor, and about 1 GB RAM); they however show that no significant penalty seems to result from the nonstandard rules of our regularized $\sqrt{3}$ refinement.

TABLE 2. Iteration history for the Poisson problem where Δ_0 is as in Figure 7 (b). We compare the linear averaging $\sqrt{3}$ subdivision BPX preconditioner with the classical BPX preconditioner.

	$\sqrt{3}$				dyadic			
J	dim	κ	residual	#iter	dim	κ	residual	#iter
1	13	3.62	1.95e-3	5	14	4.26	1.63e-3	5
2	44	5.46	1.85e-3	6	73	8.75	1.73e-3	8
3	156	8.98	1.63e-3	8	334	16.48	9.53e-4	11
4	490	13.81	7.26e-4	11	1431	27.03	4.41e-4	14
5	1553	17.08	5.18e-4	12	5928	34.05	2.39e-4	17
6	4740	23.06	3.05e-4	14	24137	39.68	1.12e-4	20
7	14488	23.40	1.79e-4	15	97418	43.68	7.60e-5	22
8	43730	27.78	9.54e-5	17	–	–	–	–
9	132021	–	6.05e-5	18	–	–	–	–

TABLE 3. Iteration history and timings for the Poisson problem, where Δ_0 is as in Figure 7 (a). We compare the linear averaging $\sqrt{3}$ subdivision MDS-BPX preconditioner with the classical MDS-BPX preconditioner.

	$\sqrt{3}$					dyadic				
J	dim	κ	residual	#iter	time (s)	dim	κ	residual	#iter	time (s)
3	28	4.43	1.64e-3	7	–	59	5.15	1.54e-3	7	–
4	92	4.95	8.12e-4	11	–	284	7.00	6.63e-4	7	0.02
5	318	6.19	3.95e-4	9	0.02	1245	8.25	5.01e-4	8	0.12
6	994	6.26	3.00e-4	10	0.06	5214	9.21	3.42e-4	9	0.53
7	3128	7.03	2.11e-4	9	0.22	21343	9.98	1.25e-4	11	4.02
8	9528	6.88	9.95e-5	11	1.75	86368	10.63	7.49e-5	12	18.84
9	29050	7.39	6.68e-5	10	3.36	–	–	–	–	–
10	87614	7.16	3.61e-5	10	25.59	–	–	–	–	–

TABLE 4. Iteration history and timings for the Poisson problem, where Δ_0 is as in Figure 7 (a). We compare the linear averaging $\sqrt{3}$ subdivision MDS-HB preconditioner with the classical MDS-HB preconditioner.

	$\sqrt{3}$					dyadic				
J	dim	κ	residual	#iter	time (s)	dim	κ	residual	#iter	time (s)
3	22	2.36	2.30e-4	3	–	49	4.58	6.56e-4	4	0.01
4	64	3.94	4.17e-4	4	–	225	10.86	8.83e-4	7	0.03
5	226	5.81	5.81e-4	5	0.02	961	19.68	4.45e-4	11	0.13
6	676	7.93	1.93e-4	7	0.06	3969	32.03	3.40e-4	14	0.58
7	2134	9.78	1.58e-4	8	0.19	16129	47.35	2.02e-4	18	4.72
8	6400	12.38	6.95e-5	10	1.59	65025	65.61	1.12e-4	23	29.36
9	19522	14.89	5.90e-5	11	3.51	–	–	–	–	–
10	58564	18.04	3.41e-5	13	24.79	–	–	–	–	–

Remark 4.1. In practical situations one would use nested iteration, i.e., in an outer iteration loop going from a sufficiently coarse resolution level to the finest resolution level J one would compute the solution at each level with the multilevel

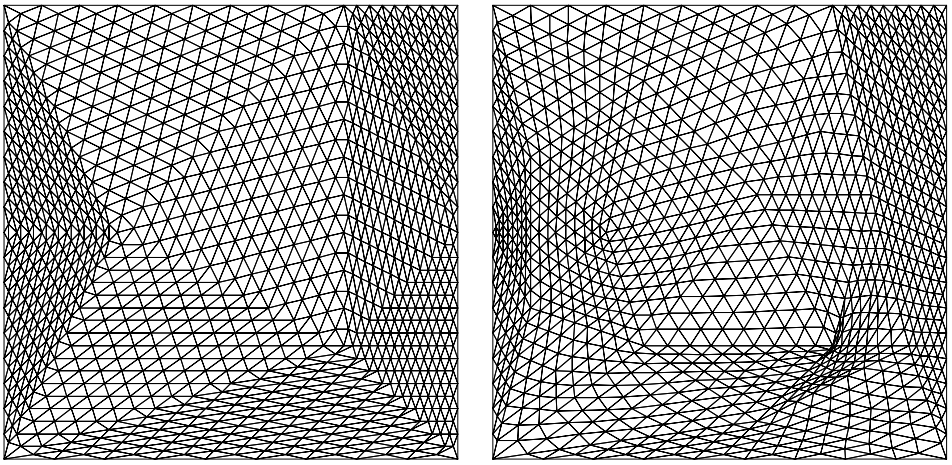

(a) Regularized $\sqrt{3}$ refinement (b) Parametric $\sqrt{3}$ refinement

FIGURE 8. We compare our regularized $\sqrt{3}$ refinement with parametric $\sqrt{3}$ refinement. We applied 5 steps of refinement to the irregular initial triangulation Δ_0 from Figure 7 (b). Parametric $\sqrt{3}$ refinement, where always the barycenters of the triangles are inserted, degenerates in this case.

preconditioned conjugate gradient method from the solution obtained at the previous coarser level as an initial guess. At each level, the internal iteration is stopped if the energy norm of the residual is comparable to the discretization error on that level. We did not use nested iteration in Tables 1–4 because our intention here was to demonstrate the full power of the preconditioners themselves.

Remark 4.2. Computing the H^1-norm of the residual r_J is easy. For an optimal preconditioner such as the BPX preconditioner one can prove that the energy norm of the residual is equivalent to the ℓ_2-norm of the residual of the preconditioned discretized system; see, e.g., [9]. Although the MDS-HB preconditioner is not an optimal preconditioner, we have also used the ℓ_2-norm of the residual in this case.

Remark 4.3. In this last remark, we provide additional motivation for using regularized $\sqrt{3}$ refinement, as adopted throughout this paper. $\sqrt{3}$ refinement was originally introduced by Kobbelt ([10]) in a parametric version; i.e., for the linear averaging rule, new interior vertices are always inserted at the barycenter of the old triangle so that the same subdivision rules apply for odd and even refinement steps (and not only for odd refinement steps as in our regularized variant). Despite its advantages in subdivision theory, the parametric approach has some serious drawbacks for our purposes here. Figure 8 shows that the parametric $\sqrt{3}$ refinement leads to a degenerate triangulation after 5 steps of refinement, due to the single pair of triangles in Δ_0 of Figure 7 (b) with an angle greater than 90 degrees. The regularized $\sqrt{3}$ refinement used throughout this paper never does degenerate, provided that Δ_0 and its first refinement Δ_1 are conforming triangulations. Moreover, it ensures that

$$\Delta_0 \to \Delta_2 \to \Delta_4 \to \cdots$$

corresponds to regular triadic refinement, which was heavily used in the analysis.

References

[1] B. Aksoylu and M. Holst, *Optimality of multilevel preconditioners for local mesh refinement in three dimensions*, SIAM J. Num. Anal. **44** (2006), 1005–1025. MR2231853 (2007d:65029)

[2] J. H. Bramble, *Multigrid methods*, Pitman Research Notes in Mathematics Series, vol. 294, Longman Scientific, 1993. MR1247694 (95b:65002)

[3] J. H. Bramble, J. E. Pasciak, and O. Steinbach, *On the stability of the L^2 projection in $H^1(\Omega)$*, Math. Comp. **71** (2002), 147–156. MR1862992 (2002h:65175)

[4] J. H. Bramble, J. E. Pasciak, and J. Xu, *Parallel multilevel preconditioners*, Math. Comp. **55** (1990), 1–22. MR1023042 (90k:65170)

[5] S. C. Brenner, *An optimal-order multigrid method for $P1$ nonconforming finite elements*, Math. Comp. **52** (1989), 1–15. MR946598 (89f:65119)

[6] ———, *An optimal-order nonconforming multigrid method for the biharmonic equation*, SIAM J. Numer. Anal. **26** (1989), 1124–1138. MR1014877 (90i:65189)

[7] ———, *Convergence of nonconforming multigrid methods without full elliptic regularity*, Math. Comp. **68** (1999), 25–53. MR1620215 (99c:65229)

[8] Z. Chen and P. Oswald, *Multigrid and multilevel methods for nonconforming Q_1 elements*, Math. Comp. **67** (1998), no. 222, 667–693. MR1451319 (98g:65118)

[9] W. Dahmen, *Wavelet and multiscale methods for operator equations*, Acta Numerica **6** (1997), 55–228. MR1489256 (98m:65102)

[10] L. Kobbelt, *$\sqrt{3}$-subdivision*, Computer Graphics Proceedings, Annual Conference Series, ACM SIGGRAPH, 2000, pp. 103–112.

[11] U. Labsik and G. Greiner, *Interpolatory $\sqrt{3}$-subdivision*, Comput. Graph. Forum **19** (2000), no. 3, 131–138.

[12] P. Oswald, *On a hierarchical basis multilevel method with nonconforming $P1$ elements*, Numer. Math. **62** (1992), 189–212. MR1165910 (93b:65059)

[13] ———, *On discrete norm estimates related to multilevel preconditioners in the finite element method*, Constructive Theory of Functions (K. G. Ivanov, P. Petrushev, and B. Sendov, eds.), Proc. Int. Conf. Varna, 1991, Bulg. Acad. Sci., Sofia, 1992, pp. 203–214.

[14] ———, *Multilevel finite element approximation: Theory and applications*, B.G. Teubner, Stuttgart, 1994. MR1312165 (95k:65110)

[15] ———, *Preconditioners for nonconforming elements*, Math. Comp. **65** (1996), 923–941. MR1333322 (96j:65056)

[16] ———, *Intergrid transfer operators and multilevel preconditioners for nonconforming discretizations*, Appl. Numer. Math. **23** (1997), 139–158. MR1438084 (98g:65110)

[17] ———, *Optimality of multilevel preconditioning for nonconforming $P1$ finite elements*, Numer. Math. **111** (2008), no. 2, 267–291. MR2456833

[18] H. Yserentant, *On the multi-level splitting of finite element spaces*, Numer. Math. **49** (1986), 379–412. MR853662 (88d:65068a)

The first author's work was done while at the Department of Computer Science, Katholieke Universiteit Leuven, Celestijnenlaan 200A, B-3001 Heverlee, Belgium

E-mail address: janm31415@gmail.com

School of Engineering and Science, Jacobs University Bremen, Campus Ring 1, 28759 Bremen, Germany.

E-mail address: p.oswald@jacobs-university.de